Locally Adaptive Color Correction for Underwater Image Dehazing and Matching

Codruta O. Ancuti[†*], Cosmin Ancuti[‡*], Christophe De Vleeschouwer[‡] and Rafael Garcia[†]
[†]Computer Vision and Robotics Group, University of Girona, Spain
[*]MEO, Universitatea Politehnica Timisoara, Romania
[‡]ICTEAM, Universite Catholique de Louvain, Belgium

Abstract

Underwater images are known to be strongly deteriorated by a combination of wavelength-dependent light attenuation and scattering. This results in complex color casts that depend both on the scene depth map and on the light spectrum. Color transfer, which is a technique of choice to counterbalance color casts, assumes stationary casts, defined by global parameters, and is therefore not directly applicable to the locally variable color casts encountered in underwater scenarios. To fill this gap, this paper introduces an original fusion-based strategy to exploit color transfer while tuning the color correction locally, as a function of the light attenuation level estimated from the red channel. The Dark Channel Prior (DCP) [16] is then used to restore the color compensated image, by inverting the simplified Koschmieder light transmission model, as for outdoor dehazing. Our technique enhances image contrast in a quite effective manner and also supports accurate transmission map estimation. Our extensive experiments also show that our color correction strongly improves the effectiveness of local keypoints matching[1].

1. Introduction

Recent years brought important research and developments of the underwater exploration based on autonomous underwater vehicles (AUV's), which have the advantage of reducing the need for human intervention with a better coverage efficiency and survey precision. AUV's have to use computer vision techniques for autonomous navigation in various applications such as underwater infrastructure inspection, marine biology research and underwater archeology. Unfortunately, employing effectively computer vision techniques in underwater is a challenging task due to the reduced visibility of the captured images. In underwater the light propagation is distorted due to the absorption and scattering, which respectively affect the energy and direction of propagated light. These distortions result in scenes with foggy appearance and poor contrast. Moreover, in underwater, the colors are faded because their composing wavelengths are cut differently according to the water depth.

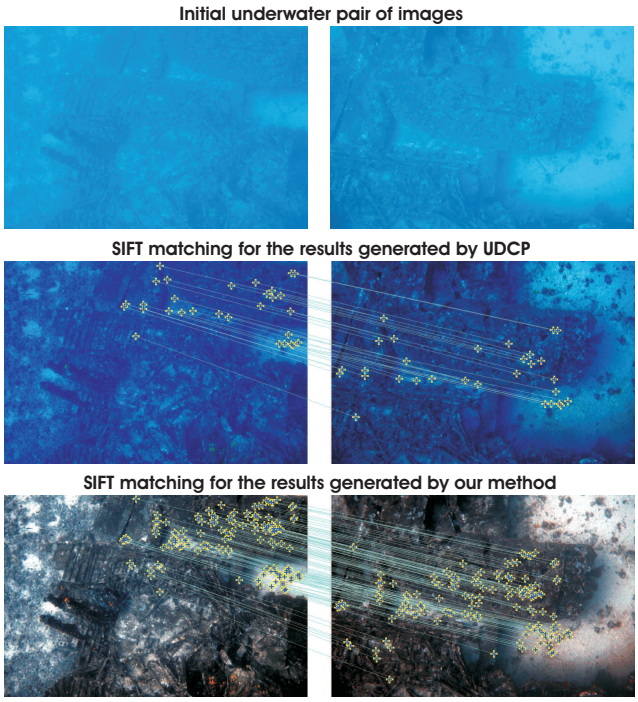

Figure 1. *No valid matches are obtained when applying the original SIFT matching procedure [25] on the original pair of underwater images (top row). In contrast, applying the same matching procedure on the images dehazed by UDCP [20] (mid row) and by our technique (bottom row) results in 30 and 135 correct matches, respectively.*

Since the deterioration of underwater scenes results from the combination of multiplicative and additive processes, enhancing the visibility in underwater is a challenging task. Single image based techniques have been introduced only recently and in general have been inspired by the outdoor dehazing strategies [9, 16, 37, 23, 1]. One of the most influ-

[1]The first two authors contributed equally to this work.

ential technique was introduced by He et al. [16] based on the Dark Channel Prior (DCP). However, due to the color dependent attenuation, underwater images can not be restored properly using DCP without initial image color spectrum restoration (see Fig. 7).

In this work we introduce an original color correction strategy as a pre-processing step to improve the conventional restoration method derived from the DCP [17]. Our color correction builds on color transfer.

Color transfer typically transfers the color mean and standard deviation from a reference image to a target image, and is known to be effective in many contexts. It is however generally admitted that the global nature of the color transfer procedure is not suited to the spatially variable color casts encountered in underwater scenes. In underwater, the color correction should ideally depend on the light attenuation level, which itself depends on the scene depth and light spectrum. Since conventional color transfer methods rely on global (and not local) image statistics, they do not have the capability to tune/adjust the color correction locally. To circumvent this limitation, we propose to adopt a fusion-based strategy, and introduce appropriate inputs and weight maps. In short, as inputs, two color images are respectively defined to compensate a small and a large color distortion. Those inputs are then blended in proportion to a weight map reflecting the desired level of color correction. In our experiments, the level of correction is defined based on the red channel intensity, which is known to provide a relevant cue to estimate the light attenuation level in underwater medium. In practice, the first image is simply the original image. It is promoted by the fusion when no color correction is needed. The second input is promoted in regions of strong attenuation. It is derived by applying a color transfer procedure to a so-called composite image that modifies the regions of weak attenuation so that their color statistics reflect the stronger attenuation encountered in the image. In that way, the color transfer parameters, which are estimated globally on the whole picture, become relevant to correct colors in the regions with significant attenuation.

Quite interestingly, our strategy appears to enhance image contrast in a quite effective manner by circumventing the wavelength-dependent color attenuation. This ability to enhance the image contrast is very useful when considering the many computer vision tasks that rely on image comparison (e.g. image matching or optical flow) and on local appearance changes (gradient-based methods like SIFT or HoG-based detectors). We demonstrate the utility of our dehazing method for the task of matching images based on local feature points using the classical SIFT operator (see Fig. 1).

Overall, the main contribution of this paper consists in using a fusion-based approach to modulate the color transfer as a function of the light attenuation, which is highly non-uniform in underwater environments. This results in improved underwater visibility, and is shown to benefit contrast-dependent computer vision tasks.

2. Related Work

A number of methods have been considered to improve the visibility of underwater images, ranging from hardware acquisition solutions to image dehazing and color correction.

Polarizing filters. The polarization-based methods rely on multiple images to generate a clear underwater image [34, 35, 38]. They use polarizing filters fixed to a camera, and vary the degree of polarization to capture several images that contain complementary information. Schechner and Averbuch [34] exploit this technique to estimate the transmission map of the underwater scenes. Polarization methods have been used also for outdoor image dehazing [36]. The polarization techniques have been shown to be effective for static scenes but, due to the multi-acquisition principle, are not applicable to dynamic acquisition.

Dark channel prior (DCP). Most of the methods investigated to restore a single underwater image have been inspired by recent outdoor dehazing strategies [9, 16, 37, 23, 1], thereby assuming that the light propagation is reasonably well approximated by the Koschmieder's model [22]. A representative example is the Dark Channel Prior (DCP). Initially introduced by He et al. for outdoor dehazing [16, 17], DCP has been extremely influential for many underwater dehazing techniques. DCP assumes that the radiance of an object in a natural scene is small in at least one of the color component, and consequently defines regions of small transmission as the ones with large minimal value of colors. For instance, the approach of Chiang and Chen [6] employs the DCP to segment the foreground and the background regions, and uses this information to remove the haze and color variations based on color compensation. Drews-Jr et al. [20] assume that the predominant source of visual information under the water lies in the blue and green color channels. The new prior Underwater Dark Channel Prior (UDCP) has been shown to be more robust than DCP to estimate the transmission for the underwater scenes. Red Channel Prior introduced by Galdran et al. [12] aims to recover colors associated with short wavelengths and is based on the assumption that, in underwater images, the red component reciprocal increases as the distance to the camera increases.

To find those image regions that are the most haze-opaque, Emberton et al. [8] designed a hierarchical rank-based method exploiting a set of features that reflect the green-blue dark channel intensity, the color channels standard deviations, and the greyscale gradient. This helps in refining the back-scattered light estimation, which in turns improves the light transmission model inversion. Lu and

al. [27] employ color lines, as in [10], to estimate the ambient light, and implement a variant of the DCP to estimate the transmission. As additional worthwhile contributions, bilateral filter is considered to remove highlighted regions before ambient light estimation, and another locally adaptive filter is considered to refine the transmission.

Our approach is also a single-image based underwater dehazing approach that builds on the Dark Channel Prior of He et al. [16]. It differentiates from previous work by implementing a simple but effective pre-processing step to correct the complex color shifts inherent to underwater images.

Color correction. Most of the methods used to balance the image colors [7] make a specific assumption to estimate the color of the light source, and then achieve color constancy by dividing each color channel by its corresponding normalized light source intensity. Among those methods, the Gray world algorithm [4] assumes that the average reflectance in the scene is achromatic. Hence, the illuminant color distribution is simply estimated by averaging each channel independently. The Max RGB [24] assumes that the maximum response in each channel is caused by a white patch [7], and consequently estimates the color of the light source by employing the maximum response of the different color channels. In their 'Shades-of-Grey' method [11], Finlayson et al. first observe that Max-RGB and Gray-World are two instantiations of the Minkowski p-norm applied to the native pixels, respectively with $p = \infty$ and $p = 1$, and propose to extend the process to arbitrary p values. The best results are obtained for $p = 6$. The Grey-Edge hypothesis of Weijer and Gevers [39] further extends this Minkowski norm framework. It assumes the average edge difference in a scene to be achromatic, and computes the scene illumination color by applying the Minkowski p-norm on the derivative structure of image channels, and not on the zero-order pixel structure, as done in Shades of Grey. Despite of its computational simplicity, this approach has been shown to obtain comparable results than state-of-the-art color constancy methods, such as the method of [14], which relies on natural image statistics. Other recent works include [2], which combines adaptive histogram equalization with global color adjustment, and [3], which accounts for perceptual aspects by adjusting the color distributions in the Ruderman opponent color space $l\alpha\beta$ [33].

Next to the methods relying on light source color estimation, the color transfer approach provides an alternative to balance colors in cases where the light source is complex. In short, color transfer manipulates the color values of a source image so that the target image shares the color statistics of a reference image. It is typically used to enhance photo-consistency [31, 30, 15, 18]. A representative example of color transfer approach that is used later in the manuscript is the simple and fast method of Reihard et al. [31]. It performs the transfer in the Ruderman et al. perception-based $l\alpha\beta$ color opponent color space [33], by shifting and scaling the pixel values of the source image to match the mean and standard deviation of the reference image. Specifically, once converted to the $l\alpha\beta$ color space [32], the transfer works independently on each component c of the color space, and we have:

$$I^c_{CT}(x) = \frac{\sigma^c_R}{\sigma^c_S}(I^c_S(x) - \bar{I}^c_S) + \bar{I}^c_R \tag{1}$$

with indices R, S, and CT referring to the reference, the source, and the color transferred images respectively. $\bar{I}^c_R$ and $\bar{I}^c_S$ denote the mean value of component c in the reference and source image, respectively. σ^c_R and σ^c_S denote the standard deviation of component c in the reference and source image, respectively.

In the underwater context, the main limitation of the above color correction methods lies in their global nature, which makes it unable to adjust the color correction to spatially varying underwater attenuation levels (which depend on depth and color spectrum). As can be seen in Fig. 2 and Fig 4, a straightforward application of conventional color balance and color transfer methods to the input image tends to over-compensate the attenuation in regions that are close to the camera (and thus less attenuated), thereby inducing reddish appearances. To adjust the color correction locally and deal with the variable and wavelength-dependent attenuation, we introduce a fusion-based approach to modulate, as a function of the estimated attenuation, the correction associated to a color transfer procedure (Section 4). The color corrected image is then restored based on the inversion (Section 5) of the simple and wavelength-independent Korshmieder light transmission model (Sections 3).

3. Underwater Light Propagation

The comprehensive studies of McGlamery [28] and Jaffe [19] have shown that the total irradiance incident on a generic point of the image plane has three main components in underwater mediums: direct component, forward scattering and back scattering.

The direct component is the light reflected directly by the target object onto the image plane. At each image coordinate vector x, the direct component is expressed as:

$$E_D(x) = J(x)e^{-\eta d(x)} = J(x)t(x) \tag{2}$$

where $J(x)$ is the radiance of the object, $d(x)$ is the distance between the observer and the object, and η is the attenuation coefficient. The exponential term $e^{-\eta d(x)}$ is also known as the transmission $t(x)$ through the underwater medium. Using the same attenuation coefficient, independently of the light wavelength, does not reflect the fact that the attenuation strongly depends on the light color in underwater environments. This severe approximation, which

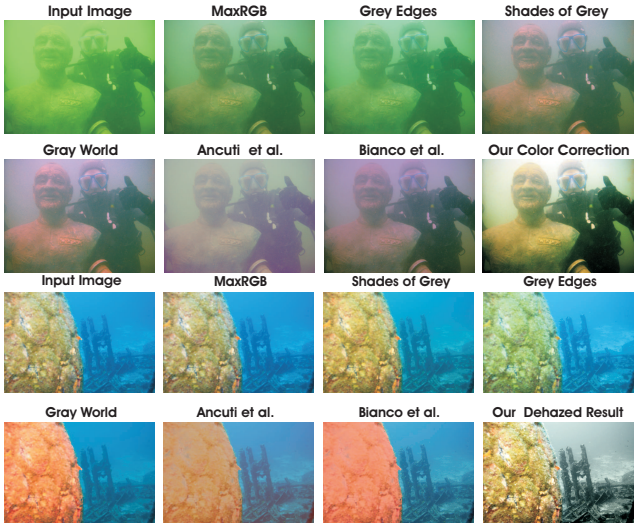

Figure 2. *Underwater color correction using several traditional white balancing techniques and the underwater techniques of Ancuti et al. [2] and Bianco et al. [3]. In the first two rows, the foreground dominates the scene and the attenuation level is relatively uniform. In contrast, in the last two rows, the scene contains objects at very different depths, inducing different attenuation levels. As a consequence, the color correction techniques of [2] and [3] result in reddish appearances because they overcompensate the attenuation in regions that are close to the camera. Our locally adaptive color correction overcomes this limitation.*

is required to invert the transmission model based on the DCP (see below), is the source of poor enhanced quality if the wavelength-dependent attenuation is not compensated in some way (see Fig.2). Our work builds on color transfer to deal with this issue.

Back-scattering acts like a glaring veil superimposed on the object. In many practical cases, back-scattering remains the principal source of contrast loss and color shifting in underwater images. Mathematically, it is often expressed as:

$$E_{BS}(x) = B_{\infty}(x)(1 - e^{-\eta d(x)}) \tag{3}$$

where $B_{\infty}(x)$ is a color vector known as the *back-scattered light*.

Forward scattering adds to the irradiance and has been found to mainly cause image blurring, with little color artifact.

Ignoring the forward scattering component, the simplified underwater optical model thus becomes:

$$I(x) = J(x)e^{-\eta d(x)} + B_{\infty}(x)(1 - e^{-\eta d(x)}) \tag{4}$$

This simplified underwater camera model (4) has a similar form than the model of Koschmieder [22], used to characterize the propagation of light in the atmosphere.

4. Underwater Color Correction

Color correction aims at improving the image aspect, primarily by removing the undesired color castings due to various illumination or medium attenuation properties. In underwater, the green-bluish appearance needs to be rectified. However, this correction is not straightforward to implement because the color distortion depends on the scene depth and on the light spectrum, as a consequence of the wavelength-dependent light attenuation.

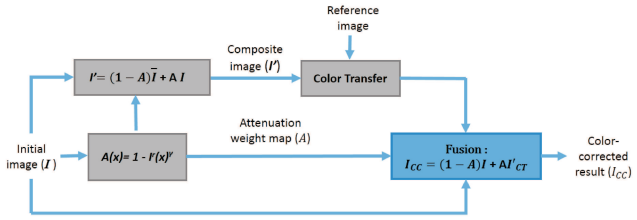

Figure 3. *Overview of our locally adaptive color correction technique. The fusion process blends two inputs according to the local attenuation level. In our experiments, the attenuation weight map $A(x)$ is estimated based on the red channel intensity. The two inputs correspond to the initial image (bottom path), and to an image in which the colors of strongly attenuated regions have been properly corrected (top path, see the text for details).*

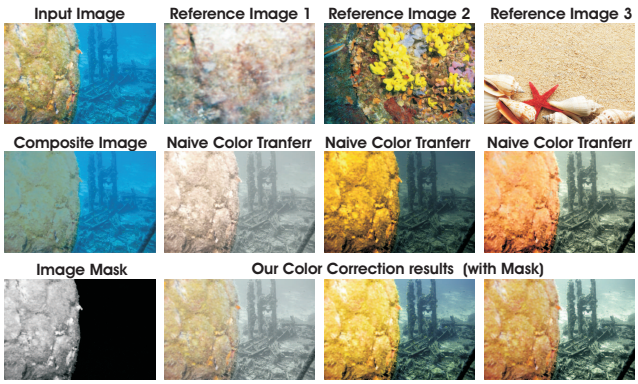

Figure 4. *Adapting our input image based on the different levels of attenuation. Compared with the naive color transfer procedure (that employs directly the initial image) our result shows better visibility with less color distortion and grain effects.*

In underwater, the color correction should ideally depend on the light attenuation level. However, conventional color correction methods rely on global (and not local) image statistics, and are thus missing the capability to tune/adjust the color adjustment locally. To circumvent this limitation, as depicted in Fig. 3, we propose to adopt a fusion-based approach to adapt the color correction locally. Therefore, we derive two inputs (one corresponding to the minimal level of correction, and the second to the maximal level of correction), and blend them in proportion to the desired level of correction, which itself corresponds to the level of light attenuation.

We now explain how the attenuation level is estimated, and how the inputs are derived.

In our experiments, the attenuation map $A(x)$ is simply estimated based on the red channel information as:

$$A(x) = 1 - I^r(x)^{\gamma} \tag{5}$$

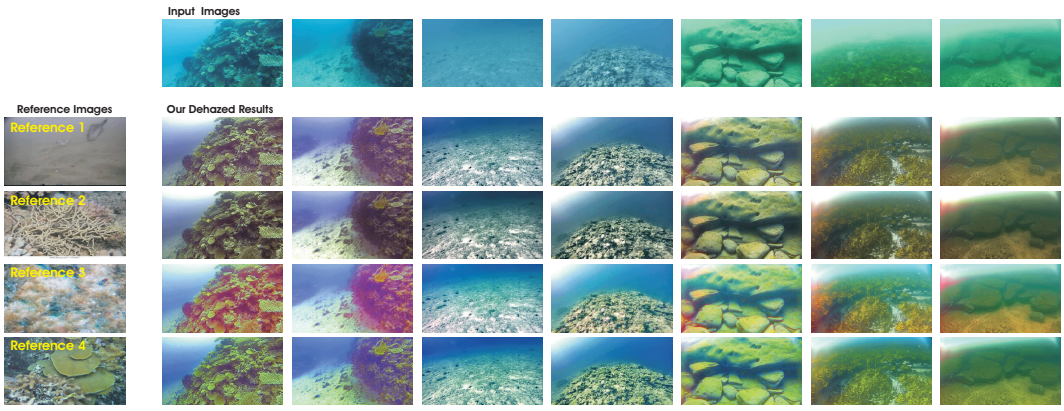

Figure 5. *Our approach performs well for various (clear underwater) reference images. As a general requirement, the reference images need to have good distribution of all color channels.*

where $I^r(x)$ represents the red channel of the initial underwater image I and γ is the parameter that controls the gamma correction in the form of power-law expression (we generate our results with the default value of $\gamma = 1.2$). This way to estimate the attenuation is motivated by several previous works [5, 12], investigating the correlation between color attenuation and red channel intensity. It is however worth mentioning that in turbid waters or in places with high concentration of plankton, the blue channel may be significantly attenuated due to absorption by organic matter. The works in [27, 26] have demonstrated the importance of accounting for the severe blue attenuation in turbid water cases. In our framework, this can be done simply by using the blue channel instead of the red channel to estimate the light attenuation level when the blue component appear to be weaker than the red in the initial image.

The first input, which is the one promoted by the fusion in absence of attenuation, is simply the initial input image, without color correction. This is because the colors remain undistorted in absence of attenuation.

The derivation of the second input is a bit more tricky. To complement the initial image (= first fusion input), it should be defined to properly correct the colors in regions that are significantly attenuated in the initial image. We propose to adopt a color transfer strategy for this purpose because it effectively corrects severe color inconsistencies between source and target image statistics, and because reference underwater images that are characterized by a proper and weakly attenuated color spectrum are easily available from numerous underwater studies (e.g. underwater vehicles acquiring images at different depths during a 2D mapping survey). To ensure that regions that are largely attenuated in the input underwater image are properly corrected in the color transferred image, the source image processed by the color transfer algorithm should be designed carefully, taking two constraints into account. First, the largely attenuated regions should remain unchanged in the source image compared to the initial underwater input, because their color corrected version are of primary interest during the subsequent fusion process. Second, the color distributions of the source image -which directly determine the global color transfer parameters- should be representative of a scene captured with significant attenuation, so that the associated color transfer parameters become appropriate/relevant to deal with largely attenuated regions.
To satisfy those two constraints, we propose to feed the global color transfer procedure with a composite image defined so that the weakly attenuated regions statistics are shifted towards the ones of regions with higher attenuation. Formally, the composite image I' is defined by:

$$I^{'}(x) = A(x)I(x) + [1 - A(x)]\bar{I} \tag{6}$$

where $\bar{I}$ is the mean value of the input image, and $A(x)$ is the attenuation map defined in (5). As can be seen in Fig.4 the foreground regions of the composite image I' tend towards the background (see Fig.4), which -as desired- pushes the global statistics of the composite image towards the statistics of the regions subject to a larger attenuation. The Reihard et al. [31] color transfer method, presented in Section 2.C, is then applied to the composite image, to generate the color transferred image $I'_{CT}(x)$, used as a second fusion input.

Given the color transferred composite image $I'_{CT}(x)$ and the initial image $I(x)$, our final color corrected image $I_{CC}(x)$ is then generated based on a straightforward fusion procedure, using the attenuation map $A(x)$ and its reciprocal $[1 - A(x)]$ to weight each input:

$$I_{CC}(x) = A(x)I^{'}_{CT}(x) + [1 - A(x)]I(x). \tag{7}$$

5. Underwater Dehazing and Transmission Estimation

To dehaze the underwater images we have built on the method of He et al. [17]. The output of the color correc-

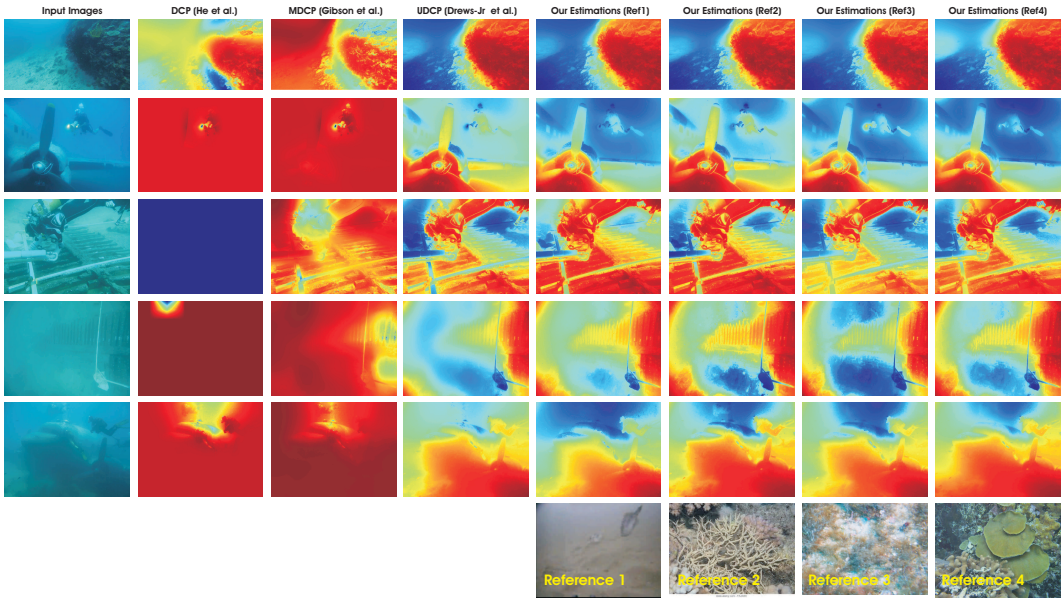

Figure 6. *Estimated transmission maps generated by different specialized underwater techniques (DCP [17], MDCP [13], UDCP [20]) and our approach generated with four different reference images.*

tion step, denoted $I_{CC}(x)$ is restored by inverting the image formation model defined by Eq. 4. Formally, when $\Omega(x)$ defines a local patch centered in x, the Dark Channel Prior [17] states that $\min_{y\in\Omega(x)}\left(\min_{c\in r,g,b} J^c/{B_\infty}^c\right) \approx 0$ for all x. Hence, based on the image formation model (4), we can estimate the transmission as:

$$t(x) = 1 - \min_{y\in\Omega(x)}\left(\min_{c\in r,g,b} I^c_{CC}(y)/{B_\infty}^c\right) \quad (8)$$

the large values of the dark channel $DC(x)$, defined as $DC(x) = min_{y\in\Omega(x)}(min_{c\in r,g,b} I^c_{CC}(y))$, correspond to locations x where $t(x)$ is close to 0, and where $I_{CC}(x) \approx B_\infty$.

To solve (8), we need to estimate B_∞. Therefore, as in [17], we observe that the DCP also implies that the large values of the dark channel $DC(x)$, defined as $DC(x) = min_{y\in\Omega(x)}(min_{c\in r,g,b} I^c_{CC}(y))$, correspond to locations x where $t(x)$ is close to 0, and where $I_{CC}(x) \approx B_\infty$. The brightest pixel among those pixels with large dark channel is chosen to estimate B_∞. Formally,

$$\begin{aligned} &B_\infty = I_{CC}(y*),\ with \\ &y* = \underset{y|DC(y)>DC^{99.9}}{\boldsymbol{arg\ max}} \left(I^r_{CC}(y) + I^g_{CC}(y) + I^b_{CC}(y)\right) \end{aligned} \quad (9)$$

where $y*$ denotes the location of the brightest pixel among those pixels whose dark channel value lies above the 99.9^{th} percentile $DC^{99.9}$, while r, g, b refer to the red, green and blue color components, respectively.

6. Results and Discussion

We have extensively tested our new technique for various underwater images (e.g. different level of bluish and greenish underwater scenes). The influence of the reference image for underwater dehazing and for estimating the transmission maps are shown in Fig. 5 and Fig. 6, respectively. As can be seen our approach is quite robust and stable when using as a reference underwater images taken in good illumination conditions, where the water attenuation is reduced. Besides presenting comparative results for estimating the transmission map and underwater dehazing in this section we demonstrate the utility of our approach for the problem of image matching based on local feature points.

6.1. Transmission Qualitative Evaluation

Following the simplified underwater optical model (4), estimating an accurate transmission map $t(x)$ is crucial to restore effectively the latent image. Here, we compare the transmission estimated by various DCP related techniques and our method. In Fig.6 we demonstrate that the transmission estimation based on our color correction approach is quite robust and is only slightly influence by the chosen reference image. Additionally, in Fig.6 we present comparative results of the estimated transmission maps using DCP, MDCP , UDCP and our approach. As can be seen our strategy is able to better estimate transmission map compared with DCP and MDCP and yields comparable results with the UDCP technique of [20]. However as discussed in the next section and shown in Fig.7, our method is more competitive to restore the visibility compared with UDCP.

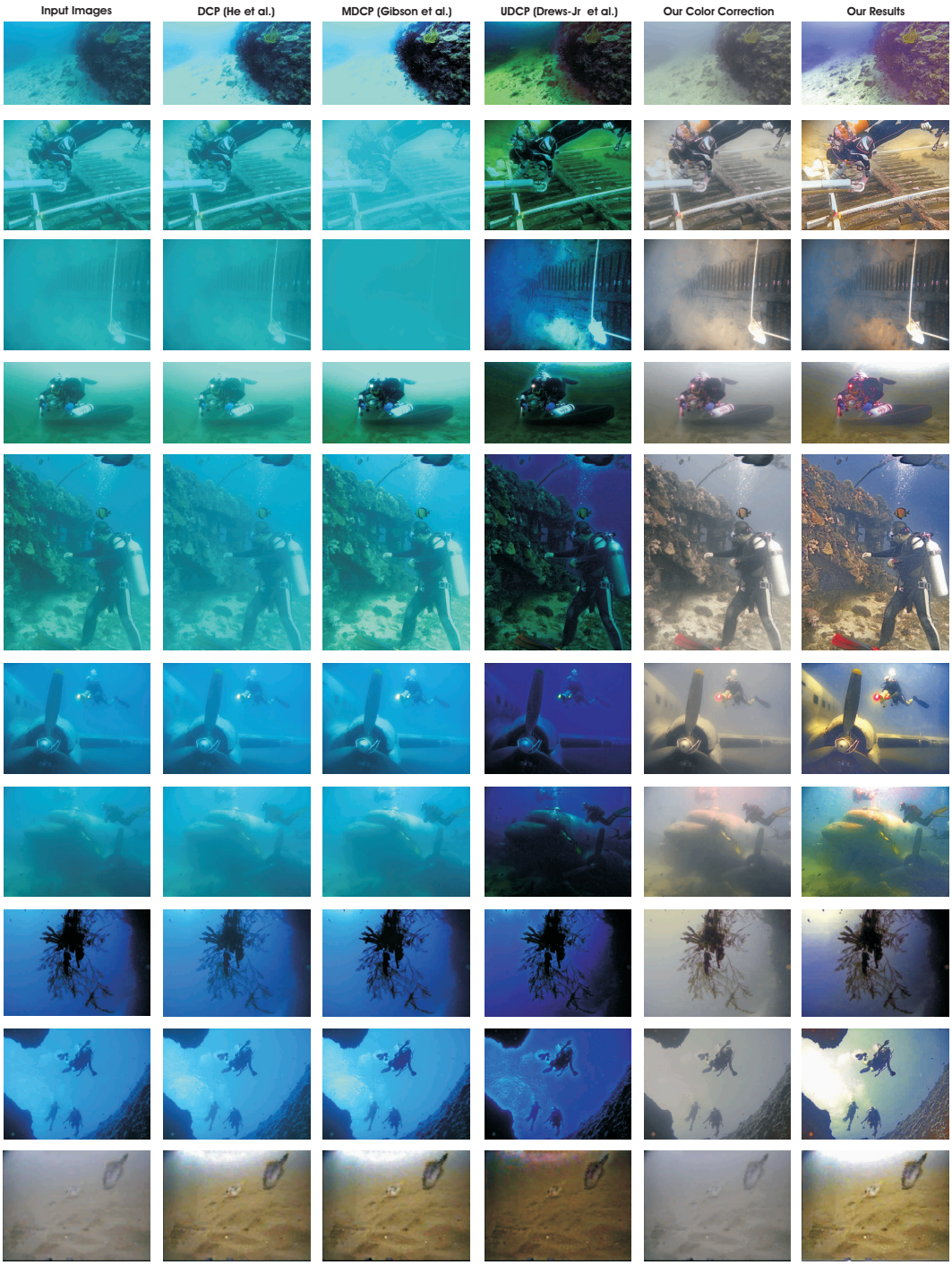

Figure 7. *Comparison to the specialized dehazing techniques: (DCP) [16], (MDCP) Gibson et al.[13] and UDCP [20]. The quantitative evaluation is shown in Table 1.*

6.2. Underwater Dehazing Evaluation

Fig.7 presents several comparative results for a set of 10 underwater images. We compare with the DCP, MDCP and UDCP dehazing techniques. As a reference image we use the first reference image presented in Fig. 5 and Fig. 6. The results have been quantitatively evaluated based on the UCIQUE [41] and PCQI [40] measures. While PCQI is a blind measure that evaluates the image contrast, UCIQUE is a specialized underwater dehazing refernceless measure (for both the larger the metrics, the better the quality). Table 1 presents the average values of UCIQUE and PCQI

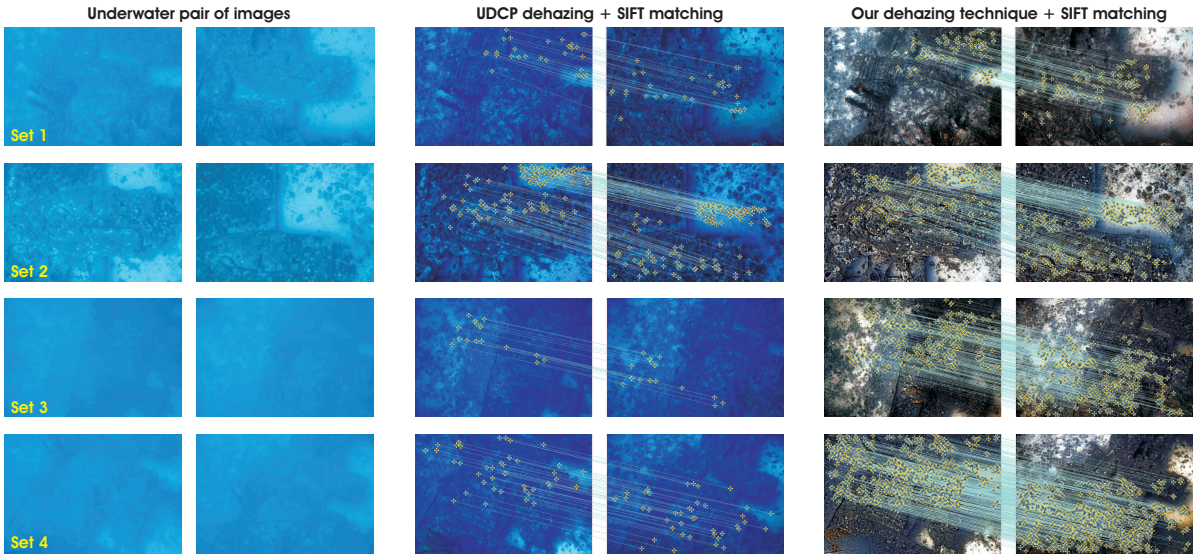

Figure 8. *Considering the 4 set of images (left) we process them by UDCP [20] (middle) and our dehazing strategy (right). The quantitative evaluation based on the SIFT matching is shown in Table 2.*

measures when applied on the 10 image results shown in Fig. 7. Visually, but also quantitatively, our dehazing method is able to yield comparative and even better outputs compared with the others analyzed techniques.

	DCP	MDCP	UDCP	Only CC	Our method
UCIQUE	0.4690	0.4927	0.5201	0.4688	0.5691
PCQI	0.9049	0.9081	0.8038	0.8417	0.9634

Table 1. *Average values of UCIQUE and PCQI of the dehazed results shown in Fig7.*

6.3. Underwater Image Matching

The effects of strong scattering in underwater adds complexity to various computer vision algorithms such as detection and localization. For instance one of the main limitation of the existing underwater SLAM (Simultaneous Localization and Mapping) techniques is due to the lack of robust, stable and local feature points that can be matched reliably in various and challenging underwater scenes [21].

We prove the utility of our technique for the task of matching images based on local feature points considering the well-known SIFT operator [25]. In our evaluation we use four challenging underwater image pairs shown in Fig 8. The evaluated images are challenging because despite of relatively simple geometry that relates them, the SIFT operator is not able to find any valid match when applied on the original underwater images.

Table 2 displays the repeatability scores [29] and the number of correct SIFT matches for the images generated by our approach and the UDCP technique [20]. As a general remark both approaches obtain similar repeatability scores. However, applying the same matching procedure [25], using our dehazed results we are able to obtain a significant additional number of valid matches compared to UDCP.

	Original		UDCP		Our Results	
	Repeat.	#correct	Repeat.	#correct	Repeat.	#correct
set 1	0	0	0.05	30	0.07	135
set 2	0	0	0.07	110	0.05	248
set 3	0	0	0.09	16	0.07	331
set 4	0	0	0.19	47	0.16	667

Table 2. *The repeatability and number of correct SIFT matches for the set of images shown in Fig8.*

7. Conclusion

In this paper we introduce a simple but effective color correction approach for underwater images. Inspired by the DCP [16] and the simple color transfer approach of [31], our comprehensive evaluation demonstrates that our strategy can effectively estimate transmission map and remove the haze effect for various underwater scenes. Moreover, we prove the utility of our dehazing method for a fundamental underwater computer vision application: matching images based on local feature points.

Acknowledgment

Part of this work has been funded by the Belgian NSF, and by a MOVE-IN Louvain, Marie Curie Fellowship. Part of this work has been funded from Marie Curie Actions of EU-FP7 under REA grant agreement no. 600388 (TECNIOspring programme), and from the Agency for Business Competitiveness of the Government of Catalonia ACCIO : TECSPR14-2-0023. Part of this work has been funded by the Belgian NSF, and by a MOVE-IN Louvain, Marie Curie Fellowship. Part of this work has been funded by the Romanian Government UEFISCDI, project PN-III-P2-2.1-PED-2016-0940. The authors would like to thank Mr. Steven Phelps and Mr. Jacob Sharvit as supporters in the water for acquiring the images of Figures 1,3,5 and 9, as well as the *URI deep sea to oculus 3D imaging* project.

References

[1] C. Ancuti and C. Ancuti. Single image dehazing by multi-scale fusion. *IEEE Transactions on Image Processing*, 22(8):3271–3282, 2013. 1, 2

[2] C. O. Ancuti, C. Ancuti, and P. Bekaert. Fusion-based restoration of the underwater images. *IEEE ICIP*, 2011. 3, 4

[3] G. Bianco, M. Muzzupappa, F. Bruno, R. Garcia, and L. Neumann. A new color correction method for underwater imaging. *International Archives of the Photogrammetry, Remote Sensing and Spatial Information Sciences*, 2015. 3, 4

[4] G. Buchsbaum. A spatial processor model for object colour perception. *Journal of The Franklin Institute*, (310):1–26, 1980. 3

[5] N. Carlevaris-Bianco, A. Mohan, and R. M. Eustice. Initial results in underwater single image dehazing. *In Proc. of IEEE OCEANS*, 2010. 5

[6] J. Y. Chiang and Y. Chen. Underwater image enhancement by wavelength compensation and dehazing. *In IEEE Trans. on Image Processing*, 2012. 2

[7] M. Ebner. *Color Constancy, Wiley 1st edition*. 2007. 3

[8] S. Emberton, L. Chittka, and A. Cavallaro. Hierarchical rank-based veiling light estimation for underwater dehazing. *Proc. of British Machine Vision Conference (BMVC)*, 2015. 2

[9] R. Fattal. Single image dehazing. *SIGGRAPH*, 2008. 1, 2

[10] R. Fattal. Dehazing using color-lines. *ACM Trans. on Graph.*, 2014. 3

[11] G. D. Finlayson and E. Trezzi. Shades of gray and colour constancy. *IS&T/SID Twelfth Color Imaging Conference: Color Science,Systems and Applications, Society for Imaging Science and Technology*, pages 37–41, 2004. 3

[12] A. Galdran, D. Pardo, A. Picon, and A. Alvarez-Gila. Automatic red-channel underwater image restoration. *Journal of Visual Communication and Image Representation*, 2015. 2, 5

[13] K. B. Gibson, D. T. Vo, and T. Q. Nguyen. An investigation of dehazing effects on image and video coding. *IEEE Transactions on Image Processing*, 2012. 6, 7

[14] A. Gijsenij and T. Gevers. Color constancy using natural image statistics and scene semantics. *IEEE Trans. Pattern Anal. Mach. Intell.*, 33(4):687–698, 2011. 3

[15] Y. Hacohen, E. Shechtman, B. Goldman, and D. Lischinski. Optimizing color consistency in photo collections. *ACM Transactions on Graphics (Proceedings of ACM SIGGRAPH 2013)*, 2013. 3

[16] K. He, J. Sun, and X. Tang. Single image haze removal using dark channel prior. *In IEEE CVPR*, 2009. 1, 2, 3, 7, 8

[17] K. He, J. Sun, and X. Tang. Single image haze removal using dark channel prior. *IEEE Trans. on Pattern Analysis and Machine Intell.*, 2011. 2, 5, 6

[18] Y. B. Hwang, J. Y. Lee, I. S. Kwon, and S. J. Kim. Color transfer using probabilistic moving least squares. *IEEE CVPR*, 2014. 3

[19] J. S. Jaffe. Computer modeling and the design of optimal underwater imaging systems. *IEEE Journal of Oceanic Engineering*, 1990. 3

[20] P. D. Jr., E. R. Nascimento, S. Botelho, and M. F. M. Campos. Underwater depth estimation and image restoration based on single images. *IEEE Computer Graphics and Applications*, 2016. 1, 2, 6, 7, 8

[21] A. Kim and R. M. Eustice. Real-time visual slam for autonomous underwater hull inspection using visual saliency. *IEEE Transactions on Robotics*, 2013. 8

[22] H. Koschmieder. Theorie der horizontalen sichtweite. In *Beitrage zur Physik der freien Atmosphare*, 1924. 2, 4

[23] L. Kratz and K. Nishino. Factorizing scene albedo and depth from a single foggy image. *ICCV*, 2009. 1, 2

[24] E. H. Land. The retinex theory of color vision. *Scientific American*, 1977. 3

[25] D. Lowe. Distinctive image features from scale-invariant keypoints. *Int. Journal of Comp. Vision*, 2004. 1, 8

[26] H. Lu, Y. Li, X. Xu, J. Li, Z. Liu, X. Li, J. Yang, and S. Serikawa. Underwater image enhancement method using weighted guided trigonometric filtering and artificial light correction. *J. Vis. Commun. Image Representation*, 2016. 5

[27] H. Lu, Y. Li, L. Zhang, and S. Serikawa. Contrast enhancement for images in turbid water. *Journal of the Optical Society of America A*, 32(5):886–893, May 2015. 3, 5

[28] B. L. McGlamery. A computer model for underwater camera systems. *Ocean Optics*, 1979. 3

[29] K. Mikolajczyk and C. Schmid. A performance evaluation of local descriptors. *IEEE TPAMI*, 2005. 8

[30] M. Oliveira, A. D. Sappa, and V. Santos. Unsupervised local color correction for coarsely registered images. *IEEE CVPR*, 2011. 3

[31] E. Reinhard, M. Adhikhim, B. Gooch, and P. Shirley. Color transfer between images. *IEEE Computer Graphics and Applications*, 2001. 3, 5, 8

[32] E. Reinhard and T. Pouli. Colour spaces for colour transfer. *Computational Color Imaging*, 2011. 3

[33] D. Ruderman, T. Cronin, and C. Chiao. Statistics of cone responses to natural images: Implications for visual coding. *J. Optical Soc. of America*, 1998. 3

[34] Y. Schechner and Y. Averbuch. Regularized image recovery in scattering media. *IEEE Trans Pattern Anal Mach Intell.*, 2007. 2

[35] Y. Y. Schechner and N. Karpel. Recovery of underwater visibility and structure by polarization analysis. *IEEE Journal of Oceanic Engineering*, 2005. 2

[36] Y. Y. Schechner, S. G. Narasimhan, and S. K. Nayar. Polarization-based vision through haze. *Applied Optics*, 2003. 2

[37] J.-P. Tarel and N. Hautiere. Fast visibility restoration from a single color or gray level image. *In IEEE ICCV*, 2009. 1, 2

[38] T. Treibitz and Y. Schechner. Active polarization descattering. *IEEE Trans Pattern Anal Mach Intell.*, 2009. 2

[39] J. van de Weijer, T. Gevers, and A. Gijsenij. Edge based color constancy. *IEEE Transactions on Image Processing*, 2007. 3

[40] L. Wang, K. Ma, and H. Yeganeh. A patch-structure representation method for quality assessment of contrast changed images. *IEEE Signal Processing Letters*, 2015. 7

[41] M. Yang and A. Sowmya. An underwater color image quality evaluation metric. *IEEE Transactions on Image Processing*, 24(12):6062 – 6071, December 2015. 7